The final authenticated version is available online at: https://doi.org/10.7567/1347-4065/ab238c

Time-Resolved Measurements of Two-Color Laser Light Emitted from GaAs/AlGaAs-Coupled Multilayer Cavity

Yasuo Minami[1]*, Kotaro Ogusu[1], Xiangmeng Lu[1], Naoto Kumagai[2], Ken Morita[3], and Takahiro Kitada[1]

[1] *Graduate School of Technology, Industrial and Social Sciences, Tokushima University, Tokushima, Tokushima 770-8506, Japan*

[2] *National Institute of Advanced Industrial Science and Technology (AIST), Nagoya, Aichi 464-8601, Japan*

[3] *Graduate School of Engineering, Chiba University, Chiba, Chiba 263-8522, Japan*

E-mail: minami@tokushima-u.ac.jp

We measured the two-color laser oscillation from a GaAs/AlGaAs-coupled multilayer cavity at 18–42 °C using current injection. We confirmed simultaneous lasing by detecting the sum frequency generation signal generated by the two-color laser light, and performed time-resolved measurement using a streak camera with a spectrometer. From the observed time transient of the spectra at various temperatures, it it is clarified that the temperature change of the device, induced by current injection, modulates the effective cavity length. Therefore, the temperature control of the device is a key factor in stable two-color lasing and THz wave generation.

1. Introduction

The terahertz (THz) wave is an electromagnetic wave whose wavelength ranges from about 10 μm to 3 mm. It is expected to be used in areas such as security and communication. Various compact THz-wave-emitting devices have been studied and developed thus far and have been constructed using semiconductor technologies, such as quantum cascade lasers (QCLs),[1–3] resonant tunneling diodes,[4,5] and photomixers.[6,7] Recently, intra-cavity difference-frequency generation (DFG) in dual-wavelength mid-infrared QCLs was attained as a THz source.[8,9] We also proposed an original THz emitter possessing a GaAs/AlAs-coupled multilayer cavity structure.[10–17] The compact device had two cavities and three distributed Bragg reflectors (DBRs), and had gain layers in the one of the cavities. By contrast, in the other cavity, DFG of the two-color laser produced in the device was performed, where the generated electromagnetic waves then exhibited THz-wave properties. The THz generating device is easy to handle because of its compactness. Moreover, the device can be manufactured without a lift-off process halfway through manufacturing as sublattice reversal in the GaAs/Ge/GaAs (113)B heterostructures was attained.[18,19)]

In this study, we performed two-color lasing in the device using the coupled multilayer cavity. Then, we observed the time transient from the two-color lasing with a streak camera and measured its dependence on the operation temperature.

2. Experiment

Using the coupled cavity structure, we fabricated a current-injection surface-emitting device, as illustrated in Fig. 1. The coupled multilayer cavity structure with InGaAs quantum wells (QWs) as the optical gain material was in the upper cavity. The upper side of the structure was epitaxially grown on 3-inch-diameter (001)-oriented GaAs substrate by molecular beam epitaxy (MBE). Therefore, the InGaAs QWs in the upper cavity as optical gain materials were grown in an (001) orientation and had a high quantum efficiency. In contrast, the lower side of the structure was epitaxially grown on a 76.2-mm-diameter (113)-oriented GaAs substrate by MBE. Therefore, the lower cavity was also grown in an (113) orientation and had a non-zero second-order nonlinear susceptibility $\chi^{(2)}$ for the light

propagating in the [113] direction,[10,11] whereas the upper cavity had a zero second-order nonlinear susceptibility. The non-zero second-order nonlinear susceptibility used in the upper cavity is required to generate THz waves in the DFG scheme. The cavity length was 1.5 wavelengths (3λ/2) for the upper and lower cavities, and the $GaAs/Al_{0.9}Ga_{0.1}As$ multilayers were grown as λ/4-DBRs. Three-period $In_{0.15}Ga_{0.85}As/GaAs$ MQWs with two different well widths of 3.6 and 4.4 nm were inserted in the upper cavity, providing a wide-range optical gain with a wavelength ranging from 910 to 940 nm,[16] and a single GaAs layer was used as the lower cavity. The structure composed of two cavities and three DBRs provides the two resonant wavelengths of about 917 and about 925 nm in this study. Be was used as a p-type dopant in the GaAs layer of the upper side of the DBR multilayer in the upper cavity, while Si was used as an n-type dopant in the GaAs layer of the lower side of the DBR multilayer in the upper cavity. The concentration of Si and Be for the DBR multilayers was about 2×10^{18} cm^{-3}. The concentration of Be for the p-contact layer was about 3×10^{19} cm^{-3}. In order to reduce the electrical resistance, each $GaAs/Al_{0.9}Ga_{0.1}As$ DBR multilayer had compositionally graded interfaces. Then, these epiwafers were connected to each other by wafer bonding,[12,14,20,21] and the optical structure part of the device was constructed. After bonding, the wafer was cut into several chips with dimensions of 18×14 mm^2. Then, the remaining (001) GaAs substrate was completely removed by mechanical polishing and selective wet etching using a citric acid-based etchant.[22] The pair layer number of the top, middle, and bottom DBRs was 28, 12.5, and 34, respectively.

We carried out the following procedure to inject current into the coupled cavity structure prepared as described above. First, we defined a circular mesa by the wet etching process, which is composed of etching of the p-type DBR, selective etching of the upper cavity, and selective etching of the topmost AlGaAs layer of the n-type DBR. The current confinement structure was formed by the horizontal-direction oxidation of a 44.1-nm-thick AlAs layer inserted in the upper cavity including MQWs. Then, the AlAs was selectively oxidized from the sidewall. In this study, the diameter of the current confinement structure was set to 60 μm. Next, n-type electrodes were formed by depositing AuGe/Ni/Au (50/12.5/50 nm) onto the exposed n-type DBR surface, and the mesa structure was buried in polyimide film. Finally, a p-type electrode with a hole for an optical window was

formed by depositing Ti/Au (5/100 nm) onto the p-type DBR surface, and rapid thermal annealing was applied. Details of the fabrication method, structure, and optical properties of the device have been described elsewhere.[16)]

A current pulse injection with a pulse width of 500 ns and repetition rate of 1 kHz or 50 kHz from the upper metal contact to the lower metal contact generated light emission in the QW cavity at near-room temperature (18–42 °C). The operating temperature was controlled using a heater set to the sample stage. Then, two-color laser light was emitted from the topside of the device through the optical window. To observe the optical properties of the prepared device, we measured the light emission from the device, the sum frequency generation (SFG) signal, the second-harmonic generation (SHG) signal generated by the light emission focused into a BBO (type-I) crystal with a spectrometer, and the time transient of the two-color lasing using a streak camera with a spectrometer. The experimental setup for the measurement is illustrated in Fig. 2.

3. Results and discussion

The light emission properties of the device were studied using a pulsed-current source. Figure 3(a) shows the emission spectrum measured using a spectrometer with a thermoelectrically cooled Si charge-coupled device (CCD) array. The pulse current was 290 mA with a time duration of 500 ns and repetition rate of 1 kHz. The atmospheric temperature was 24 °C. Two sharp peaks originating from the cavity modes are clearly observed in the measured spectra with wavelengths of 917 and 925 nm. The emission spectra were measured with the current range of 10–300 mA. Then, the I–L curves of the two peaks were obtained by extracting the intensities of the two peaks in the spectra, which are shown in Fig. 3(b). The threshold behaviors are clearly observed in the I–L curves, and the threshold current of about 50 mA is almost the same for the two wavelengths. However, saturation of the emission intensity of the short-wavelength mode is seen at currents above 150 mA.

Simultaneous two-color lasing in the device is crucial for efficient THz generation via the DFG process. Therefore, we carried out the SFG measurements using the configuration illustrated in Fig. 2 with the BBO crystal. When a BBO (type I) crystal is irradiated with a simultaneous two-color laser beam, not only two SHG signals but also an SFG signal can be

observed.[23] A blue band-pass filter was inserted to prevent the injection of fundamental two-color laser light into the optical fiber. Figure 3(c) shows the measured spectrum when the device was operated at a current of 290 mA with a pulse duration of 500 ns and repetition rate of 50 kHz to enhance the weak SFG and SHG signals. As shown in Fig. 3(c), an SFG signal is clearly observed between the two SHG signals, indicating simultaneous two-color lasing in the device. However, the SFG signal intensity is weaker than the expected value from the SHG signal intensities. The reduced SFG signal might be due to the different temporal profiles of the two lasing peaks in the pulse duration. Therefore, time-resolved measurement of the two-color laser emission using a streak camera with a spectrometer was performed. Figure 4 shows the measured time-resolved spectra. The injection current, pulse duration, and repetition rate were 290 mA, 500 ns, and 1 kHz, respectively. The operating temperature of the heater was maintained at 18 °C (Fig. 4(a)), 24 °C (Fig. 4(b)), 30 °C (Fig. 4(c)), and 42 °C (Fig. 4(d)), and the atmospheric temperature was 18 °C. As can be seen in Fig. 4(b), the short-wavelength mode exhibits stronger emission in the initial stage, and the emission intensity of the long-wavelength mode increases with the time delay, which induced the saturation of the emission intensity of the short-wavelength mode observed in Fig. 3(b). The offset in the emission timing among the two-color lasing is also observed in the figure, which induced the reduction of the SFG signal described above. As seen in Fig. 4, as the operating temperature increases, the emission intensity of the short-wavelength mode increases compared to that of the long-wavelength mode, resulting from the change in balance of the effective cavity length between the upper cavity and lower cavity due to the temperature-controlling heater, which was set to the stage below the lower cavity. The slight change in balance of the effective cavity lengths significantly changes the properties of the two resonant modes. In this case, the effective length of the lower cavity becomes longer with the temperature compared to that of the upper cavity. The temperature dependences of the wavelengths of the two modes at the time = 0.3 μs shown in Fig. 4 are shown in Fig. 5. In the figure, the temperature dependences of the effective cavity-length changes are also indicated by lines that can be expressed as

$$\lambda = \lambda_0 \left(1 + \frac{\alpha}{n_0} \Delta T \right), \quad (1)$$

where λ_0 is the wavelength, which is set to that at 18 °C, α is the temperature

coefficient of the refractive index of GaAs, n_0 (= 3.57) is the refractive index of GaAs for the wavelength of about 920 nm at room temperature,[24] and ΔT is the temperature change. The lines in the figure represent the best-fit lines for the experimental data. From the gradient of the lines, the temperature coefficient of the refractive index is obtained to be 3.00×10^{-4} and 2.55×10^{-4} °C^{-1}. These values agree with those estimated elsewhere;[25,26] therefore, the change in oscillation wavelength is induced by the change in effective cavity length induced by the increase in temperature. In Fig. 4(b), the wavelength of the long mode changes from 922.48 nm (time = 0.3 μs) to 922.97 nm (time = 0.7 μs) in 0.4 μs; therefore, the temperature change of the cavity is estimated to be +7 °C from Eq. (1). The increase in temperature induced by the current injection induces the change in balance of the effective cavity length between the upper cavity and lower cavity, resulting in the modulation of the oscillation wavelengths and their transient redshifts.

4. Conclusions

We demonstrated two-color lasing from a wafer-bonded GaAs/AlGaAs-coupled multilayer cavity at 18–42 °C by current injection. The coupled cavity structure was fabricated by the direct bonding of (001) and (113)B epitaxial wafers prepared individually by MBE. Then, the lasing properties of the two modes were observed under a pulsed current condition. In the experiment, the SFG signal was clearly observed, which implies that the two-color laser light from the sample was simultaneously generated in the device. THz waves with a frequency of 2.67 THz would be generated during the overlapping time of the two-color lasers via the DFG scheme in the device. However, the intensity of the SFG signal was weaker than expected. To determine why, time-resolved spectra were observed using a streak camera, which clarified the slight offset in timing among the two-color lasing. Furthermore, from the time-resolved spectra measurement at various temperatures, it was clarified that the increase in temperature of the device induced by the current injection would also induce the offset in the timing among the two-color lasing. Therefore, the temperature control of the device is a key factor in stable two-color lasing and THz wave generation.

Acknowledgments

This work was supported in part by the Grants-in-Aid for Scientific Research (KAKENHI, Nos. 16H04351 and 16K06266) from the Japan Society for the Promotion of Science (JSPS).

References

1) R. Köhler, A. Tredicucci, F. Beltram, H. E. Beere, E. H. Linfield, A. G. Davies, D. A. Ritchie, R. C. Iotti, and F. Rossi, Nature **417**, 156 (2002).
2) B. S. Williams, Nat. Photonics **1**, 517 (2007).
3) M. A. Belkin, J. A. Fan, S. Hormoz, F. Capasso, S. P. Khanna, M. Lachab, A. G. Davies, and E. H. Linfield, Opt. Express **16**, 3242 (2008).
4) M. Asada, S. Suzuki, and N. Kishimoto, Jpn. J. Appl. Phys. **47**, 4375 (2008).
5) S. Suzuki, M. Asada, A. Teranishi, H. Sugiyama, and H. Yokoyama, Appl. Phys. Lett. **97**, 242102 (2010).
6) S. Matsuura, M. Tani, and K. Sakai, Appl. Phys. Lett. **70,** 559 (1997).
7) H. Ito, F. Nakajima, T. Furuta, K. Yoshino, and T. Ishibashi, Electron. Lett. **39**, 1828 (2003).
8) K. Vijayraghavan, Y. Jiang, M. Jang, A. Jiang, K. Choutagunta, A. Vizbaras, F. Demmerle, G. Boehm, M. C. Amann, and M. A. Belkin, Nat. Commun. **4**, 2021 (2013).
9) K. Fujita, M. Hitaka, A. Ito, T. Edamura, M. Yamanishi, S. Jung, and M. A. Belkin, Appl. Phys. Lett. **106**, 251104 (2015).
10) C. Harayama, S. Katoh, Y. Nakagawa, K. Morita, T. Kitada, and T. Isu, Jpn. J. Appl. Phys. **53**, 04EG11 (2014).
11) C. Harayama, S. Katoh, Y. Nakagawa, X. M. Lu, N. Kumagai, T. Kitada, and T. Isu, Jpn. J. Appl. Phys. **54**, 04DG10 (2015).
12) H. Ota, X. M. Lu, N. Kumagai, T. Kitada, and T. Isu, Jpn. J. Appl. Phys. **55**, 04EH09 (2016).
13) T. Kitada, H. Ota, X. M. Lu, N. Kumagai, and T. Isu, Appl. Phys. Express **9**, 111201 (2016).
14) T. Kitada, H. Ota, X. M. Lu, N. Kumagai, and T. Isu, IEICE Trans. Electron. **E100-C**, 171 (2017).
15) X. M. Lu, H. Ota, N. Kumagai, Y. Minami, T. Kitada, and T. Isu, J. Cryst. Growth **477**, 249 (2017).
16) Y. Minami, H. Ota, X. M. Lu, N. Kumagai, T. Kitada, and T. Isu, Jpn. J. Appl. Phys. **56**, 04CH01 (2017).
17) T. Kitada, X. M. Lu, Y. Minami, N. Kumagai, and K. Morita, Jpn. J. Appl. Phys. **57**,

04FH03 (2018).

18) X. M. Lu, N. Kumagai, Y. Minami, and T. Kitada, Appl. Phys. Express **11**, 015501 (2018).

19) X. M. Lu, N. Kumagai, Y. Minami, and T. Kitada, Jpn. J. Appl. Phys. **57**, 04FH07 (2018).

20) T. R. Chung, L. Yang, N. Hosoda, H. Takagi, and T. Suga, Appl. Surf. Sci. **117–118**, 808 (1997).

21) H. Takagi, K. Kikuchi, R. Maeda, T. R. Chung, and T. Suga, Appl. Phys. Lett. **68**, 2222 (1996).

22) T. Kanbara, S. Nakano, S. Yano, K. Morita, T. Kitada, and T. Isu, Jpn. J. Appl. Phys. **48**, 04C105 (2009).

23) R. W. Boyd, *Nonlinear Optics* (Academic Press, London, 2008) 3rd ed., Chap. 1.

24) E. D. Palik, *Handbook of Optical Constants of Solids* (Academic Press, London, 1985), Part 2.

25) J. Talghader and J. S. Smith, Appl. Phys. Lett., **66**, 335 (1995).

26) O. Madelung, *Semiconductors: Data Handbook* (Springer, Berlin, 2004) 3rd ed., Chap. 2.

Figure Captions

Fig. 1. (Color online) Cross-section of the two-color laser generation device composed of GaAs/AlGaAs-coupled multilayer cavities fabricated in our study.

Fig. 2. (Color online) Setup of the optical system for two-color lasing measurement, SHG and SFG measurement using a BBO crystal and band-pass filter, and time-resolved measurement using a streak camera with a spectrometer.

Fig. 3. (Color online) (a) Two-color lasing spectrum. The pulse current was 290 mA with a time duration of 500 ns and repetition rate of 1 kHz. (b) I–L curves of two peaks obtained by extracting the intensities of the two peaks in (a). Red solid and blue open circles represent the long mode and short mode, respectively. (c) SFG and SHG signals generated via the BBO crystal. The pulse current was 290 mA, the pulse duration was 500 ns, and the repetition rate was 50 kHz.

Fig. 4. (Color online) Time-resolved spectra of two-color laser emission observed using a streak camera with spectrometer. The injection current, pulse duration, and repetition rate were 290 mA, 500 ns, and 1 kHz, respectively. The operating temperatures were (a) 18 °C, (b) 24 °C, (c) 30 °C, and (d) 42 °C.

Fig. 5. (Color online) Temperature dependences of wavelengths of the two modes at the time = 0.3 μs shown in Fig. 4. Red solid and blue open circles represent the long mode and short mode, respectively.

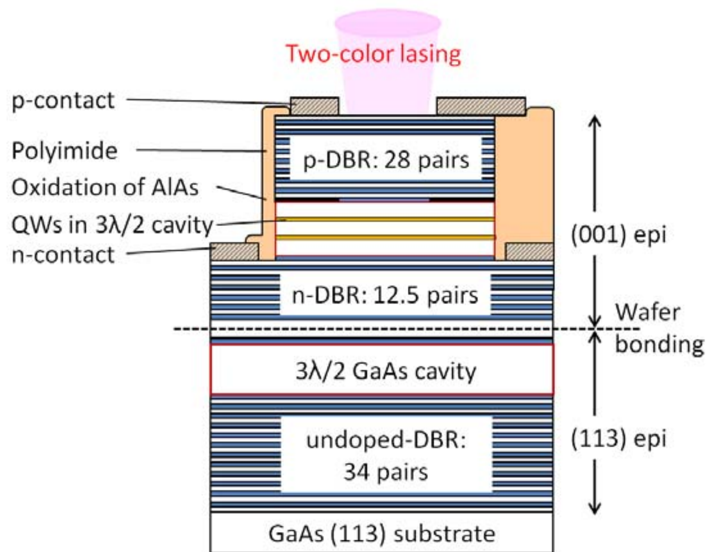

Fig. 1.

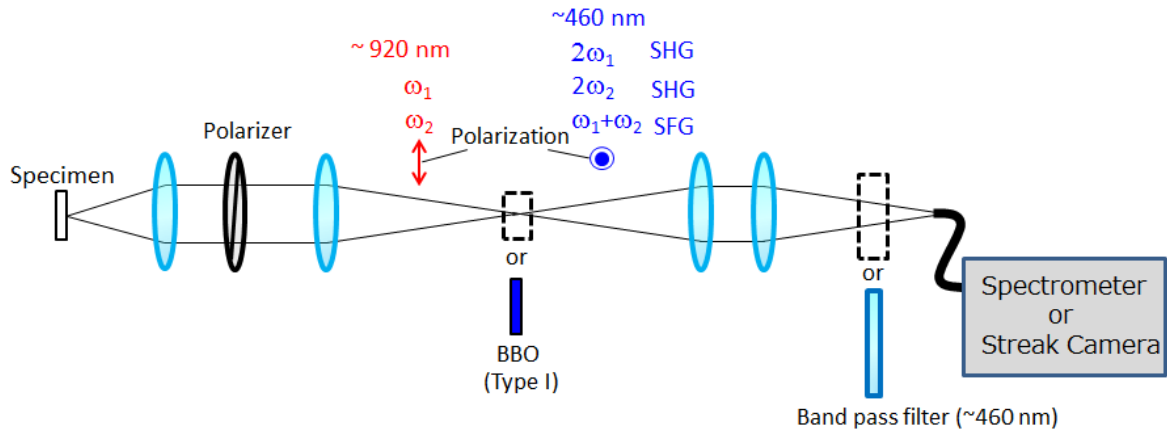

Fig. 2.

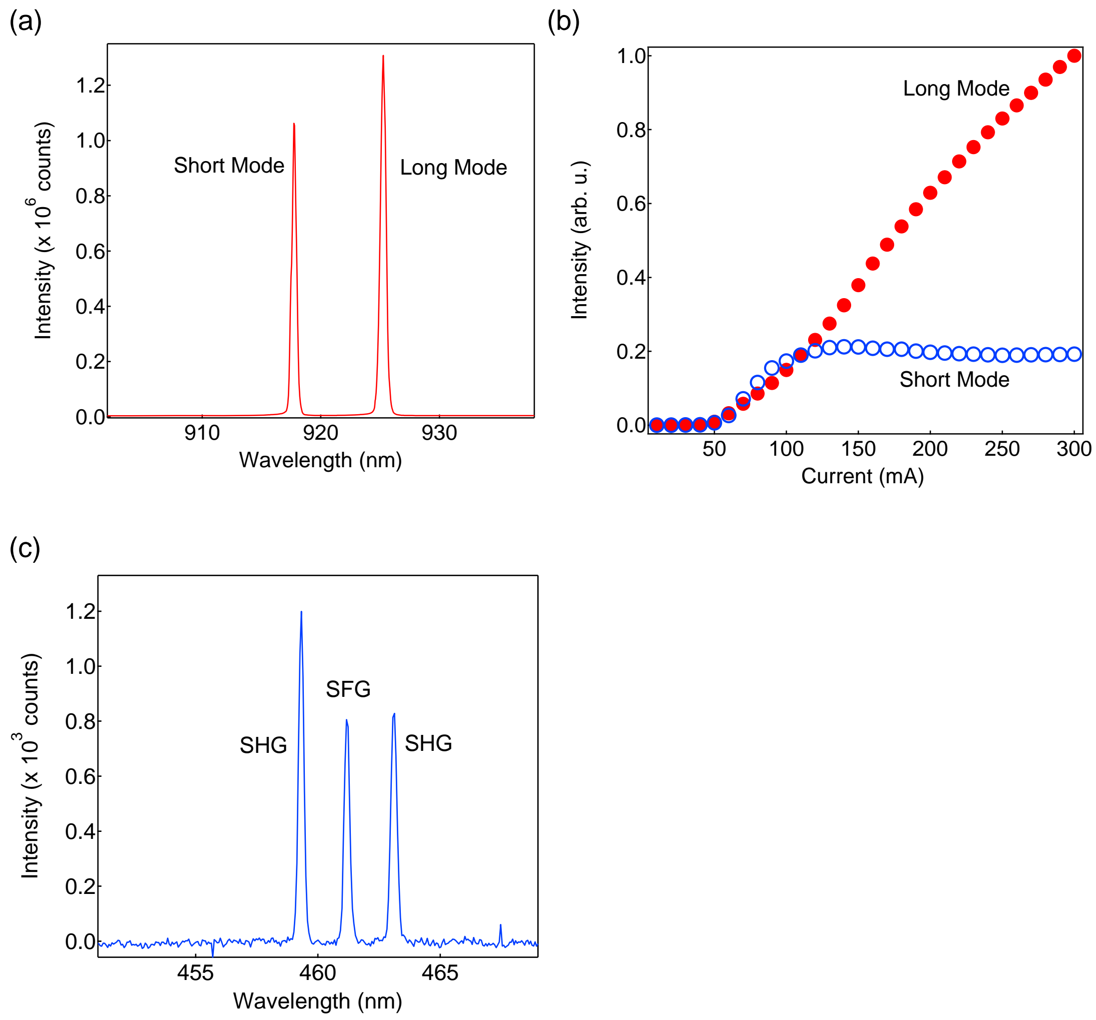

Fig. 3

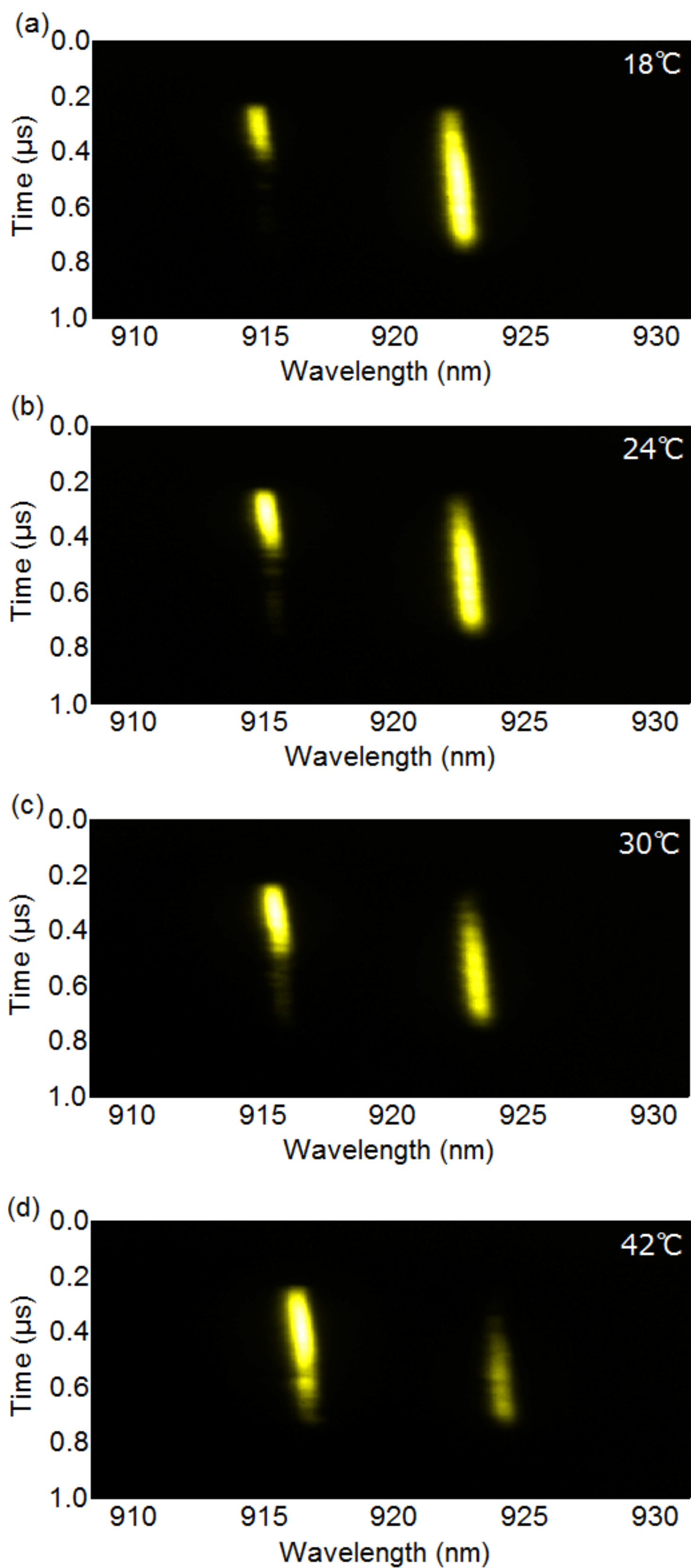

Fig. 4

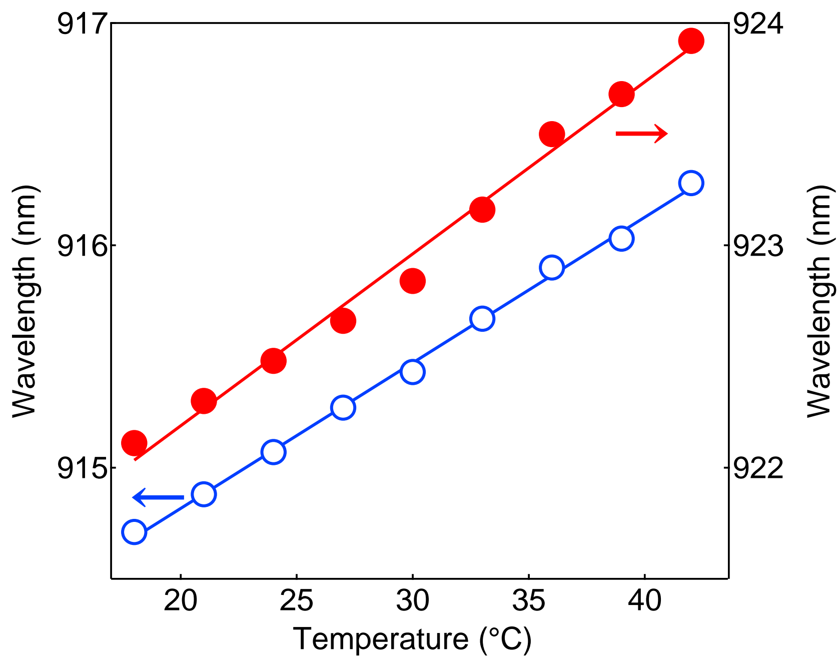

Fig. 5